Supplementary Materials **Table of Contents**

Supplementary Figure 6. Mass isotopomer distribution of metabolites used for MFA.

Supplementary Figure 7. Comparison of the measured and calculated mass distributions from optimized flux distribution by MFA

Supplementary Figure 8. Complementation of the xylose-utilizing ability of *talAB pfkA* mutant by *Lactococcus lactis pfk*

Supplementary Figure 9. Metabolic pathway models used in MFA

Supplementary Figure 10. Pathways of glucose and gluconate utilization in *zwf* and *rpe* deletion strains

Supplementary Table I. genes and enzymes mentioned
Supplementary Table II. growth and symulation datas (a separate file)
Supplementary Table III. transcript and metabolite levels (a separate file)
Supplementary Table IV. Mass isotopomer distribution, MFA models and results (a separate file)
Supplementary Table V. Strains
Supplementary Table VI. Carbon sources
Supplementary Table VII. Changes to EC_*i*AF1260_flux2 (Feist *et al*, 2007) for FBA analysis

Supplementary text 1

R5P is a precursor of nucleotides, and thus R5P synthesis is essential for cell growth. In the *zwf* mutant utilizing glucose (and most other carbon sources), flux toward R5P production is limited to the non-oxidative branch of the pentose phosphate pathway and should be synthesized via reverse flux of the transaldolase (*tal*) and transketolase (*tkt*) reactions (Supplementary Fig. 10A). Also, reverse flux of ribulose phosphate 3-epimerase (*rpe*) is critical for this single mutant, since *rpe* is a sole reaction that consumes Xu5P in the central carbon metabolism. Therefore, an additional deletion in *rpe* stops all routes for R5P synthesis (Supplementary Fig. 10C). In comparison, when the carbon source is gluconate, which enters into central carbon metabolism at 6PG, R5P is produced, as shown in Supplementary Figure 10D. Although both *tkt* and *tal* react toward synthesis of E4P, the molecule could be consumed as a source of aromatic amino acids and other metabolites, which enables the *rpe zwf* mutant to grow on gluconate. Consumption of E4P is also necessary for the *rpe* mutant to grow on glucose (Supplementary Fig. 10 D).

Supplementary Referenses

Becker SA, Feist AM, et al. (2007) Quantitative prediction of cellular metabolism with constraint-based models: the COBRA Toolbox. *Nature protocols* **2**: 727-738.

Feist AM, Henry CS, et al. (2007) A genome-scale metabolic reconstruction for Escherichia coli K-12 MG1655 that accounts for 1260 ORFs and thermodynamic information. *Mol Syst Biol* **3**: 121.

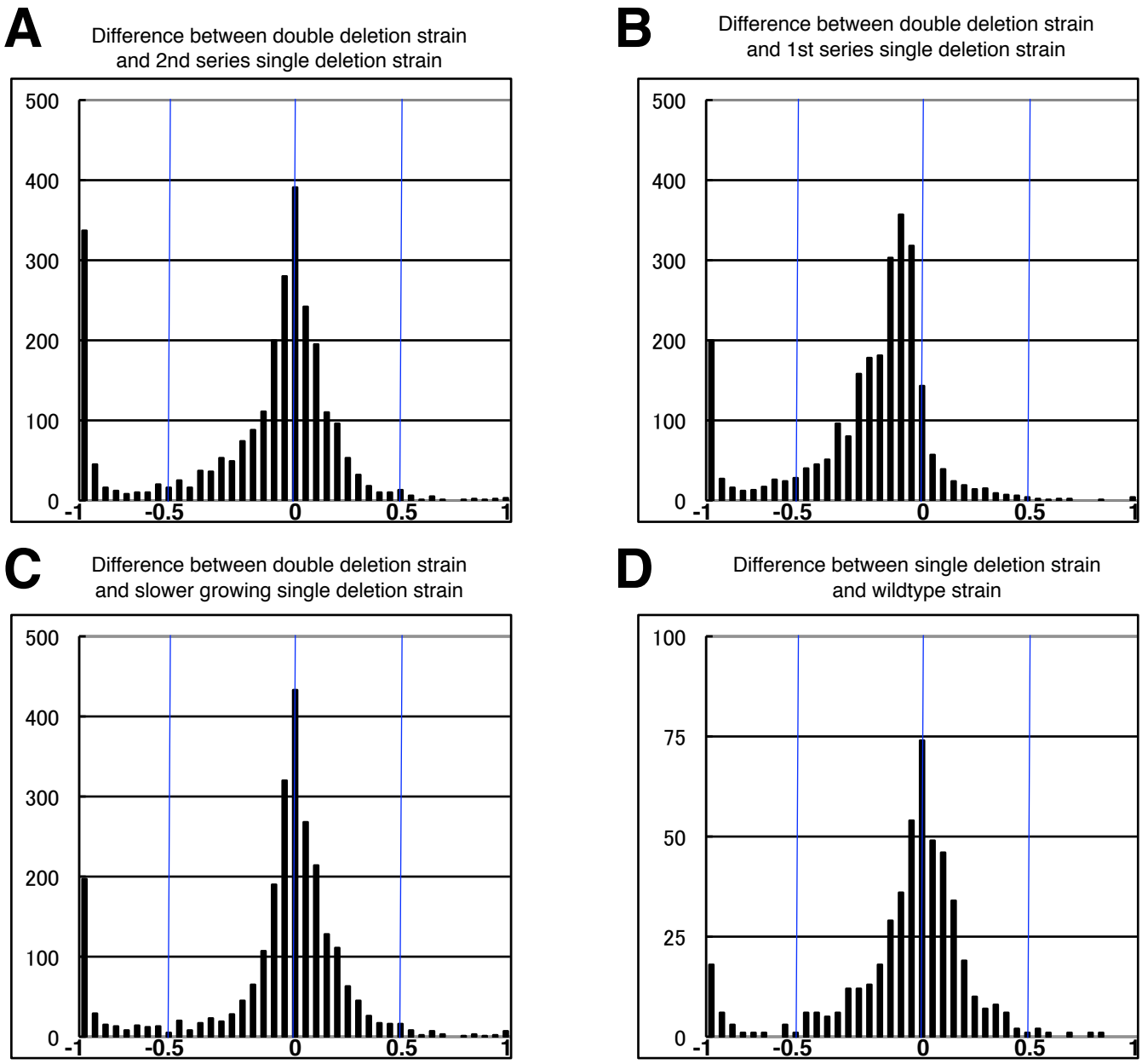

Supplementary Figure 1
Difference of growth between deletion strain and parental strains.

Histogram showing difference of relative growth between mutant strain and its parental strain were shown. (A) Difference between double deletion and single deletion in second deletion, W(x,y) – W(wt,y). (B) Difference between double deletion and single deletion in first deletion, W(x,y) – W(x,wt). (C) Difference between double deletion and slower growing single deletion, W(x,y) – min[W(x,wt) and W(wt,y)]. (D) Difference between single deletion and wild type, W(x,wt) – W(wt,wt) and W(wt,y) – W(wt,wt).

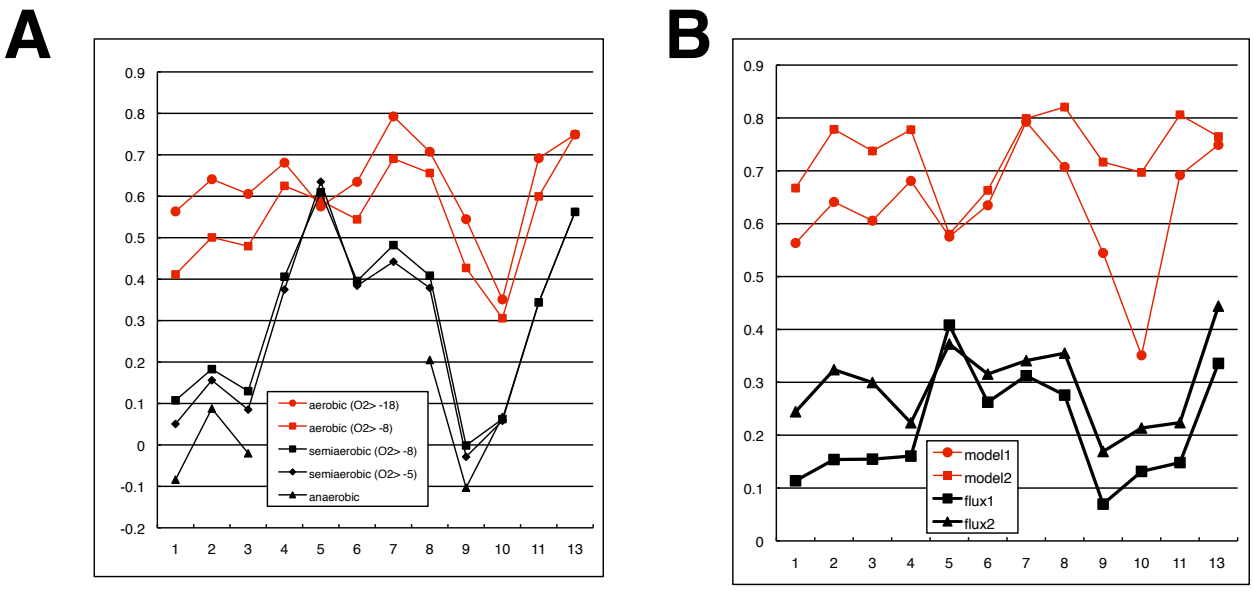

Supplementary Figure 2. Correlation coefficient between experimental result and FBA simulation

Correlation coefficient between experimental result (OD600 at 24h) and result of FBA (μ) in each medium. Numbers for each medium shown in Figure 2 are indicated in X-axis.

(A) Several different constraints reflecting gene expression of anaerobic and aerobic condition (anaerobic, semi aerobic, and aerobic) and different maximum O_2 consumption (0 to 18 mmol/g cell dry weight /hour) were used for FBA and compared with the experimental result. See Supplementary text 2 for constraints used for each FBA condition. In anaerobic condition (O_2 consumption = 0), all strains were predicted to exhibit no growth in some medium, thus cerebration coefficient was not calculated for these medium.

(B) Comparison of the result on aerobic O_2 consumption < 18, but with different model. flux1: EC_*i*AF1260_flux1 without further constraint (Feist et al, 2007), flux2: EC_*i*AF1260_flux2, based on aerobic glucose condition (Feist et al, 2007), model1: model and constraint used for first round FBA of double knockout, model2: using model with the novel reactions and with additional constraints found by the analysis of double knockout in this work.

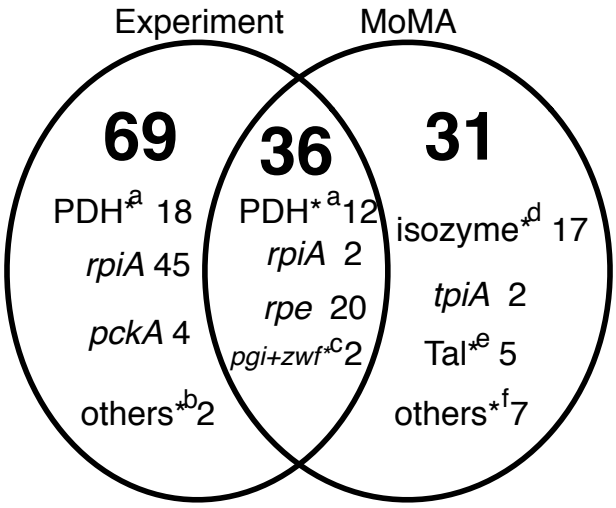

Supplementary Figure 3. Experimental and MoMA simulated conditions indicating synthetic slow-growth phenotype

To evaluate the predicted growth of a mutant strain against its parental strain, we defined RGIs-MoMA score similarly to the RGIe score used to evaluate the experimental data. Predicted growth by MoMA was used instead of the OD600 for RGIe score calculation, and the RGIs scores were calculated for 1968 cases among 2465 for which we calculated the RGIe score of the double knockout strains. The results obtained in complete medium (205) were not used for the prediction. In addition, the RGIs scores of the double mutants were not calculated when one of the parental single deletions was predicted to show no growth (292), large difference from the corresponding fraction by FBA prediction was due to single deletion to one of the PDH complex subunits, which are predicted to show no growth by MoMA. Within the 1968 cases, 105 of the 229 cases that showed synthetic slow-growth phenotype in experiment were included, excluding the 8 cases in complete medium, 111 cases in PDH related mutants, 4 cases in rpiA related mutants and one case of pfkA-Tal mutant.

Within the 1968 cases that both RGIe and RGIs-MoMA scores were obtained, number of the cases that showed synthetic slow-growth phenotype in either of experiment, MoMA, or both of experiment and MoMA are shown. Each class was subdivided into categories and the number of cases in each category is also shown. Most of the categories were defined by the first deletion, and the first deletion is indicated. Other categories were marked by *. *[a]; either of *aceE*, *aceF*, or *lpdA* in the first deletion. *[b]; one each case of *tpiA-Pyk*-glucose and *icdA-pgi*-acetate. *[c]; *zwf-pgi* and *pgi-zwf* on glucose. *[d]; cases genes of the first deletion was encoding the major isozyme. *[e]; cases having Tal as second deletion and explained by the novel reactions. *[f]; 4 cases of *icdA-aceA* on non-fermentable carbon sources, *maeB-pgi*-xylose, and *rpe-pgi*-xylose. Cases classified into the each category were shown in Supplementary Table II.

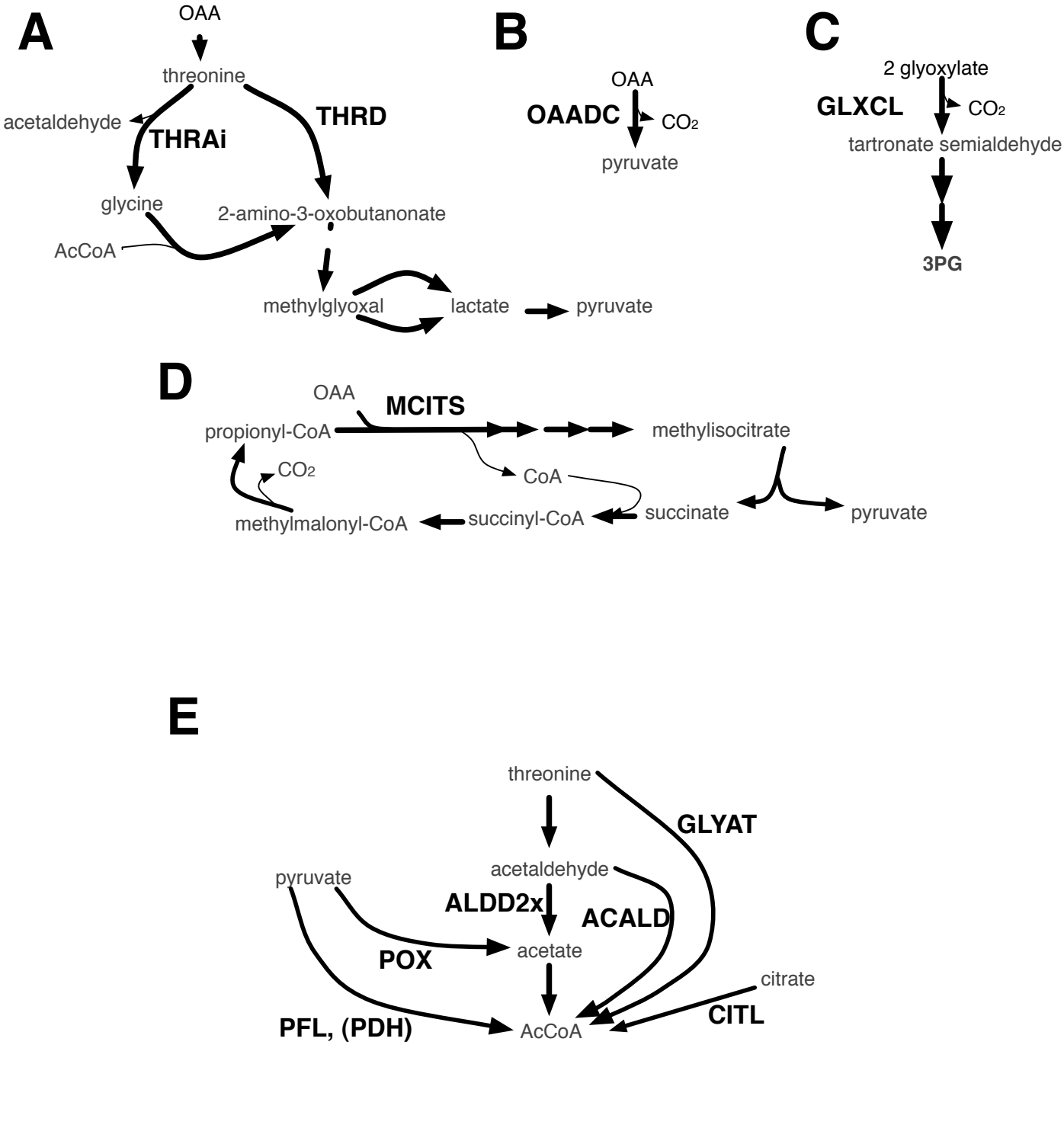

Supplementary Figure 4. Possible alternative route from TCA cycle to glycolysis (A-D), and reactions producing AcCoA (E)

(A-D) Reactions in *i*AF1260, that can connect from metabolites in TCA cycle to metabolites in glycolysis. Name of reactions used in *i*AF1260 are indicated.

(E) Reactions in *i*AF1260, that could support the growth of PDH mutants by producing AcCoA. Name of reaction used in *i*AF1260 is indicated on the arrow showing the reaction.

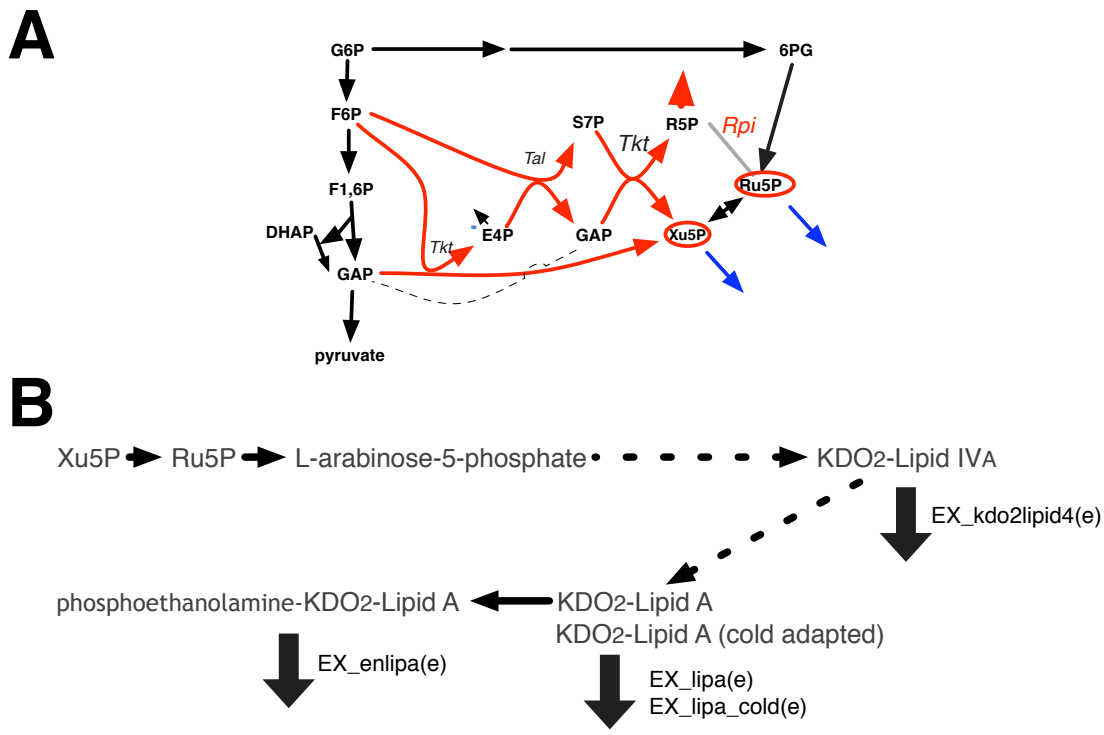

Supplementary Figure 5. Possible route of growth supporting growth of *rpi* mutants

(A) Diagram showing the flux direction in pentose phosphate pathway in *rpi* mutant. Reactions shown in red are forced by the requirement of R5P for producing necessary metabolites. Exiting flux from Xu5P or Ru5P, blue arrow, will be required to allow flux exiting from R5P.
(B) A pathway for production of lipidA related molecules and their export. The names of export reactions in *i*AF1260 are shown along with the arrows.

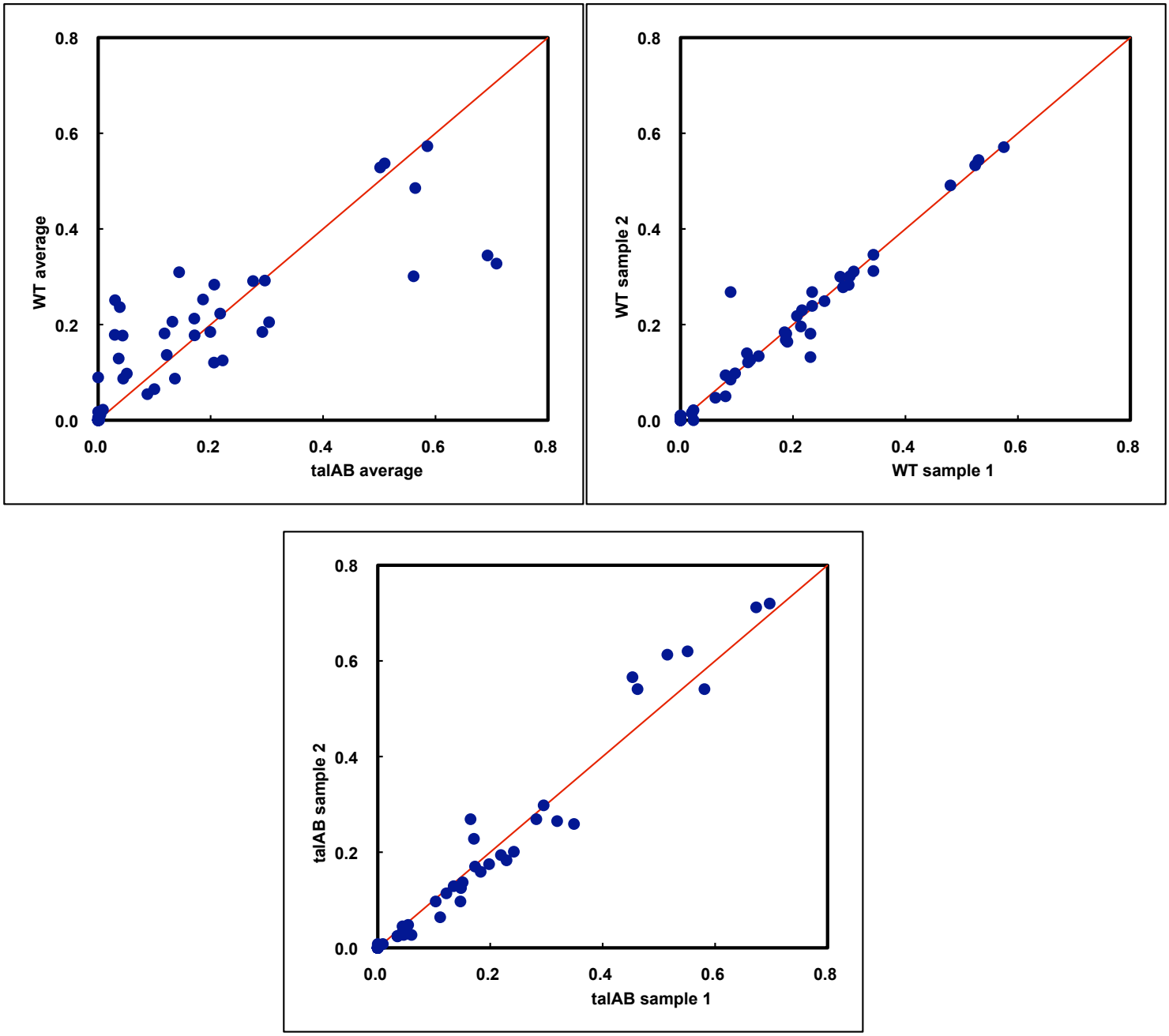

Supplementary Figure 6. Mass isotopomer distribution of metabolites used for MFA. Mass isotopomer distributions of F6P, F16P, DHAP, 3GP, Ru5P, R5P, S7P, and S17P as shown in Supplementary Table IVA are plotted. A dot indicates the relative amount of each mass isotopomer when the total amount of mass isotopomers of a metabolite is set to one. WT1, WT2, talAB1, and talAB2 are individual results from two experiments using wildtype or talA talB cells. WT: an average amount from two wildtype samples, talAB: an average amount from two talA talB samples.

Wild type-Authentic pathway model

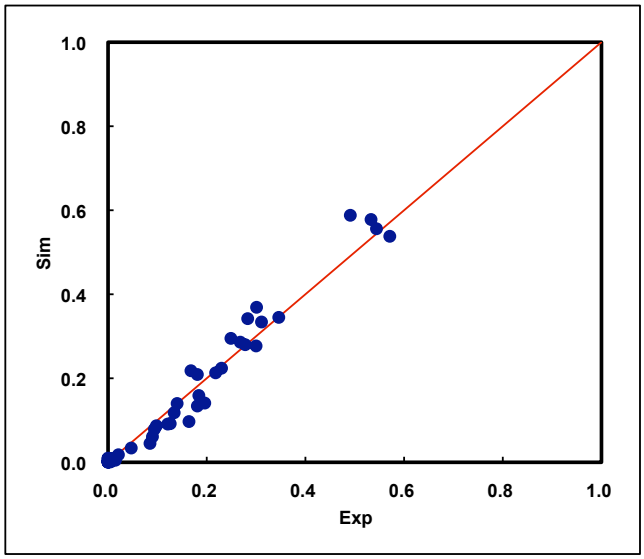

talA talB-Authentic pathway model

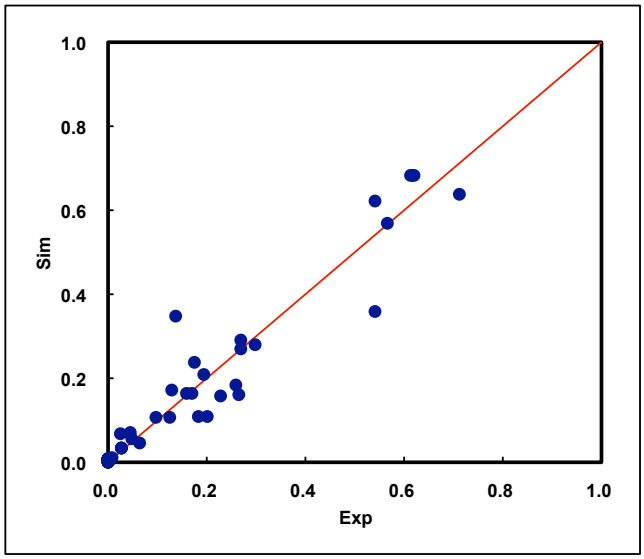

Wild type-Novel pathway model

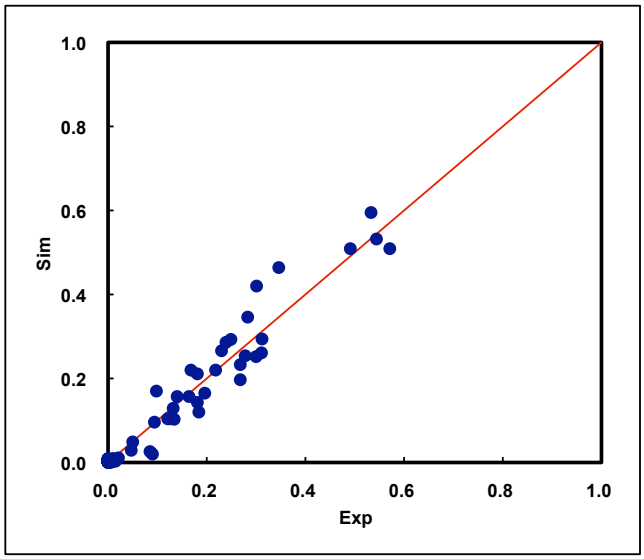

talA talB-Novel pathway model

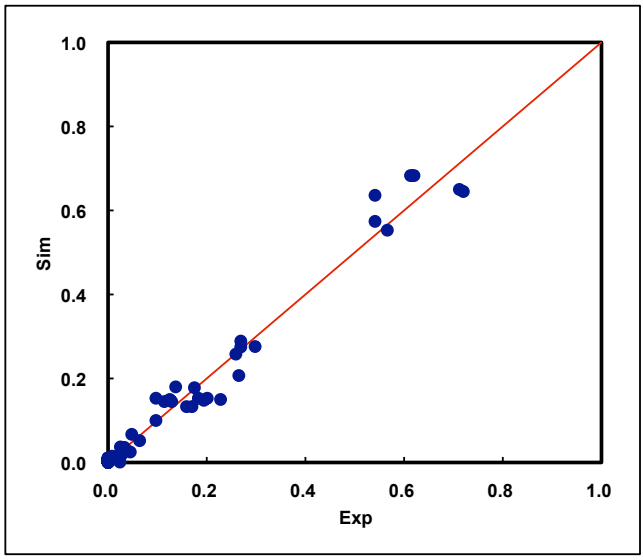

talA talB-L-type pathway model

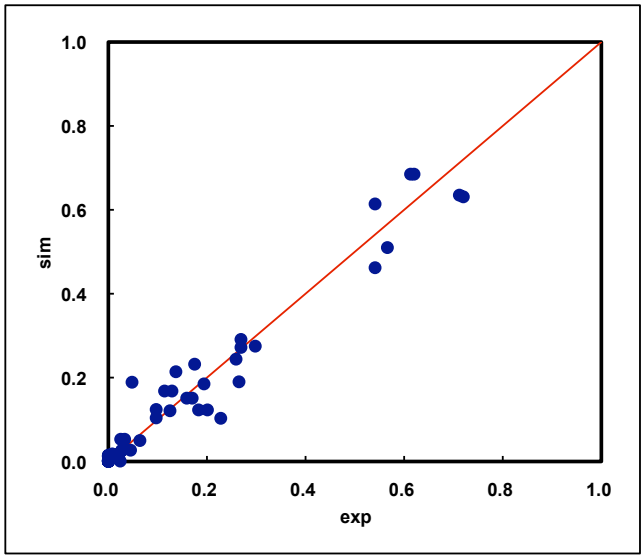

Supplementary Figure 7. Comparison of the measured and calculated mass distributions from optimized flux distribution by MFA. Each panel shows the measured (X-axis) and calculated (Y-axis) amounts of each mass isotopomer. Each value on the Y-axis was calculated from the optimized flux, as shown in Supplementary Table IV B and C.

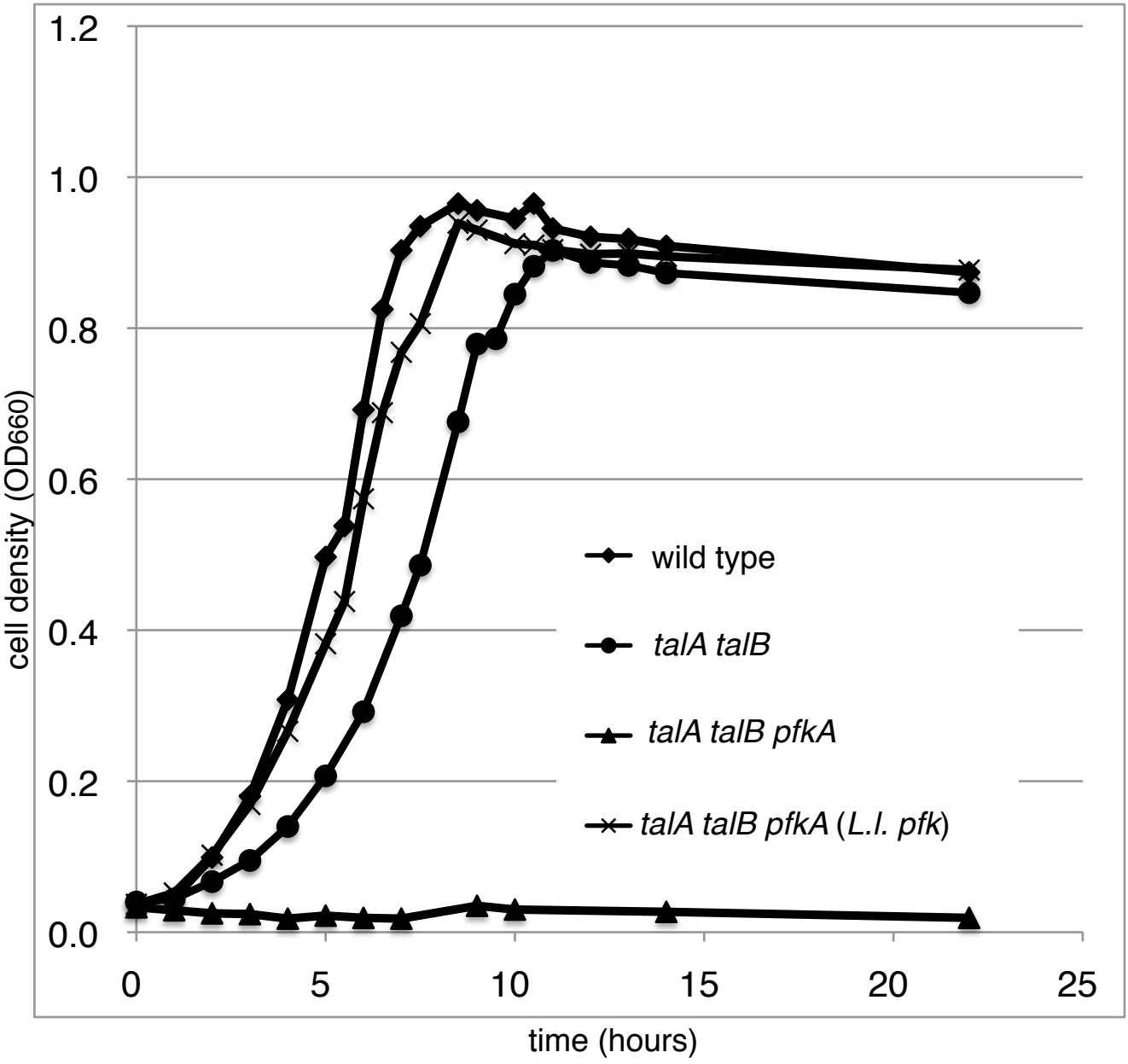

Supplementary Figure 8. Complementation of the xylose-utilizing ability of *talA talB pfkA* mutant by *Lactococcus lactis pfk*.

The entire coding region of *pfk* was amplified from the *Lacococcus lactis* genome and cloned into pTRC99A under the inducible trc promoter. The *talA talB pfkA* triple mutant was transformed with the *pfk* plasmid or pTRC99A vector, and other strains were transformed with the pTRC99A vector. The transformed cells were incubated in MOPS medium supplemented with 0.2% xylose and 1 mM IPTG. Growth (OD660) was monitored by use of miniphoto 518R (Titec, JAPAN).

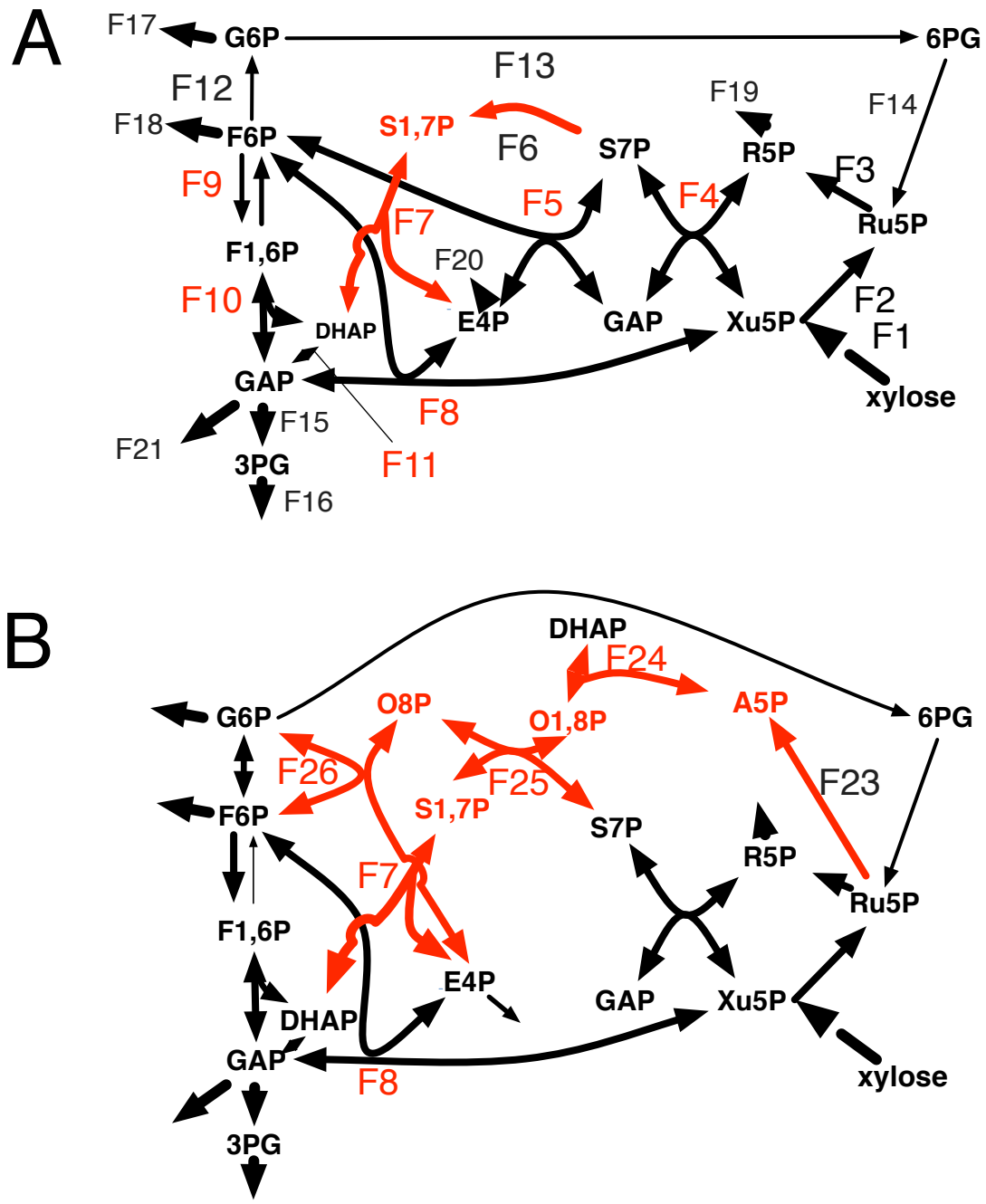

Supplementary Figure 9. Metabolic pathway models used in MFA.
Fluxes considered in the analysis are shown on the metabolic map. Bidirectional reactions are indicated by red symbols. Reactions and metabolites indicated in red are not present in the current metabolic pathway. Model (A) was used for most of the analyses, and model (B) was used to evaluate the L-type pentose phosphate pathway. See Supplementary Table IV B-D for details.

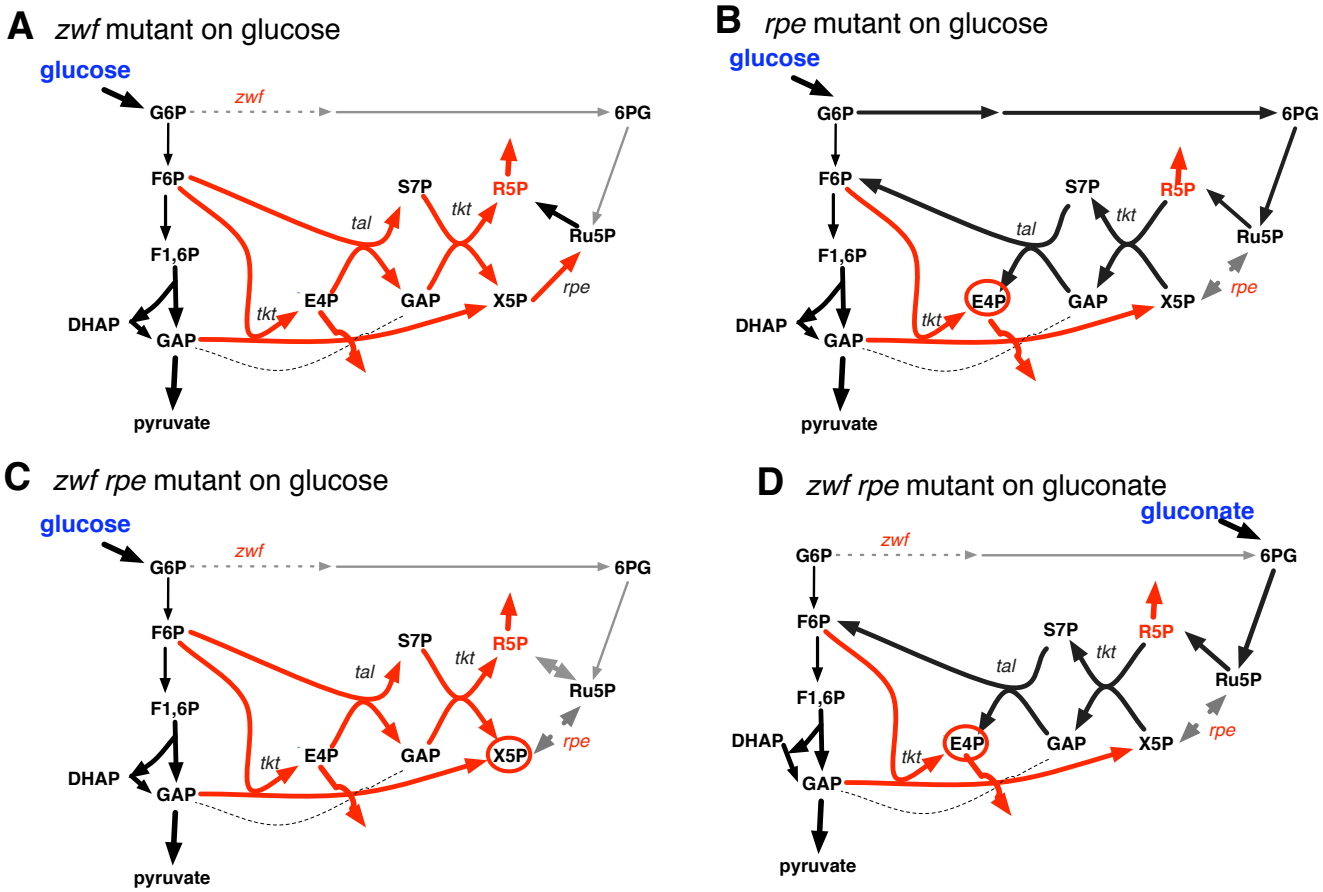

Supplementary Figure 10. Pathways of glucose and gluconate utilization in *zwf* and *rpe* deletion strains.
Part of the glycolysis and the entire pentose phosphate pathway are shown. Reactions are shown with arrows and reversed reactions, as compared with the wildtype strain grown in glucose, are shown in red. Important reactions are marked with the respective gene symbols (*zwf*, *rpe*, *tkt and tal*).

Supplementary Table 1
genes and enzymes
mentioned

gene name	gene name (Ecocyc)	product	iAF1260	first deletion	second deletion
glycolysis/gluconeogenesis					
glk	glk	glucokinase	HEX1	x	
pgi	pgi	phosphoglucose isomerase	PGI	x	pgi
pfkA	pfkA	6-phosphofructokinase I	PFK	x	
pfkB	pfkB	6-phosphofructokinase II	PFK	x	
fbaA	fbaA	fructose bisphosphate aldolase class II	FBA		
fbaB	fbaB	fructose bisphosphate aldolase class I	FBA	x	
tpiA	tpiA	triose phosphate isomerase	TPI	x	
gpmA	gpmA	phosphoglyceromutase 1	PGM	x	
gpmB	ytjC	phosphoglycerate mutase 2	PGM	x	
gpmI	gpmM	phosphoglycerate mutase, cofactor independent	PGM	x	
pykA	pykA	pyruvate kinase II	PYK	x	Pyk
pykF	pykF	pyruvate kinase I	PYK	x	Pyk
fbp	fbp	fructose-1,6-bisphosphatase I	FBP	x	
ppsA	pps	phosphoenolpyruvate synthase	PPS	x	
pentose phosphate pathway					
zwf	zwf	glucose 6-phosphate-1-dehydrogenase	G6PDH2r	x	zwf
gnd	gnd	6-phosphogluconate dehydrogenase (decarboxylating)	GND	x	
rpe	rpe	ribulose phosphate 3-epimerase	RPE	x	
rpiA	rpiA	ribose-5-phosphate isomerase A	RPI	x	
rpiB	rpiB	allose-6-phosphate isomerase / ribose-5-phosphate isomerase B	RPI	x	
tktA	tktA	transketolase I	TKT1, TKT2	x	
tktB	tktB	transketolase II	TKT1, TKT2	x	
talA	talA	transaldolase A	TALA	x	Tal
talB	talB	transaldolase B	TALA	x	Tal
acetyl-CoA production and TCA cycle					
aceE	aceE	pyruvate dehydrogenase (E1p)	PDH	x	
aceF	aceF	pyruvate dehydrogenase (lipoate)	PDH	x	
lpdA	lpd	pyruvate dehydrogenase (E3), etc	PDH, GLYCL, AKGDH	x	
gltA	gltA	citrate synthase	CS	x	
icdA	icd	isocitrate dehydrogenase-P	ICDHyr	x	
anaplerotic pathway					
pckA	pck	phosphoenolpyruvate carboxykinase (ATP)	PPCK	x	ppc_pckA
ppc	ppc	phosphoenolpyruvate carboxylase	PPC	x	ppc_pckA
sfcA	maeA	malate dehydrogenase, NAD-requiring	ME1	x	ME
maeB	maeB	malate dehydrogenase (oxaloacetate-decarboxylating) (NADP+)	ME2	x	ME
glyoxylate cycle					
aceA	aceA	isocitrate lyase	ICL		aceA
other					
deoB	deoB	phosphopentomutase	PPM2, PPM		
deoC	deoC	deoxyribose-phosphate aldolase	DRPA		
mgsA	mgsA	methylglyoxal synthase	MGSA		
control					
rrnH	–	16S, 23S and 5s rRNA and tRNA-ile and tRNA-ara(one copy of seven rRNA operons)		x	

gene name	gene name usd in this work
gene name (Ecocyc)	gene name used in EcoCyc
product	name of the gene product
iAF1260	reaction name in iAF1260
first deletion	marked as "x" when deletion of this gene was used as one of parental deletion (recipient of P1 transduction)
second deletion	Name of the second deletion series are shown when deletion of this gene was used as a donor of P1 transduction.

Supplementary Table V. Strains

parent	deletion	primer*	template
BW25113	zwf:Cm	keio	pKD13Cm
BW25113	pgi:tet	keio	pKD13Tet
BW25113	aceA:Cm	keio	pKD13Cm
BW25113	ppc:tet	keio	pKD13Tet
BW25113	sfcA:tet	keio	pKD13Tet
BW25113	talA:tet	keio	pKD13Tet
BW25113	pykA:tet	keio	pKD13Tet
BW25113	pckA:Cm	keio	pKD13Cm
BW25113	maeB:Cm	keio	pKD13Cm
BW25113	talB:Cm	keio	pKD13Cm
BW25113	pykF:Cm	keio	pKD13Cm
BW25113	rrnH:Km	new	pKD13
JE5530	P1lpa:Km	new	pKD13

* keio; primer used for keio strains, new; designed for this work

Supplementary Table VI. Carbon sources

1. Glucose: 0.4%

2. Mannitol: 0.4%

3. Fructose: 0.4%

4. Glycerol: 0.5% (v/v)

5. Acetate: sodium acetate 0.5%

6. Succinate: sodium succinate 0.5%

7. Glutamate: sodium glutamate 0.5%

8. Glucuronate: sodium glucuronate 0.5%

9. Gluconate: sodium gluconate 0.5%

10. Xylose: 0.4%

11. S+Glycerol: glycerol: 0.5% (v/v) and sodium succinate 0.5%

13. MOPS+C: no carbon source (except for casamino acid)

Supplementary Table VII. Changes to Ec_iAF1260_flux2

reaction	lower bound[a]	upper bound[b]	workaround for[c]
A Parameters for first FBA			
general (all analysis)			
F6PA	0	0	tpiA
G2PD2	-0.2		tpiA
EDD	0	0	tpiA
GLCDpp	0	0	tpiA
MGSA		0.25	tpiA
DRPA		0.25	tpiA
ASPK		0.5	aceE, aceF, lpdA
ACALD		0.1	aceE, aceF, lpdA
POX		0.1	aceE, aceF, lpdA
ALDD2x		0.1	aceE, aceF, lpdA
CITL		0.1	aceE, aceF, lpdA
GLYAT	-0.1		aceE, aceF, lpdA
carbon sources			
any_type	-6		
Casamino Acid			
ala	-0.21		
arg	-0.08		
asp	-0.22		
cys	0		
glu	-0.62		
gly	-0.12		
his	-0.07		
ile	-0.18		
leu	-0.22		
lys	-0.23		
met	-0.05		
phe	-0.12		
pro	-0.41		
ser	-0.11		
thr	-0.08		
trp	0		
tyr	-0.01		
val	-0.28		
Carbon source specific changes considering direction of the reaction			
glucose			
PGI	-0.1		d
carbon-sources entering into TCA and glycolysis after F1,6P			
TKT2		0.1	d
glycerol			
G3PD5		100	e
G3PD6		100	e
G3PD7		100	e
GLYK		100	e
Acetate			
ACS		100	e
Acetate, succinate, glutamate,			
ICL		100	e
MALS		100	e
Glucuronate, Gluconate			
G6PDH2r		1	d
Xylose			
XYLI1		100	e
XYLK		100	e
XYLabcpp		100	e
RPE		0.1	d
TKT1	-0.1		d
TKT2	-0.1		d

Cont. to next page

Supplementary Table VII. Changes to Ec_iAF1260_flux2 (cont. from previous page)

reaction	lower bound[a]	upper bound[b]	workaround for[c]
B Constraints used for testing anaerobic and semi-aerobic condition [f]			
(CADVtpp, DMSOR1, DMSOR2, FRD2, FRD3, HYD1pp, … HYD2pp, HYD3pp, NO2t2rpp, NTRIR2x, PFL,RNTR1c,… RNTR2c, RNTR3c, RNTR4c, TMAOR1, TMAOR2)…		100	
NO2t2rpp	-100		
CYTBO3_4pp		0	
C Parameters for second FBA applying feedback from double deletion analysis [g]			
MGSA		0, 0.5[h]	tpiA
DRPA		0	tpiA
THRD	0	0	*pckA*-ME
THRAi	0	0	*pckA*-ME
OAADC	0	0	*pckA*-ME
MCITS	0	0	*pckA*-ME
GLXCL	0	0	*pckA*-ME
EX_kdo2lipid4(e)	0	0	*rpiA*
EX_lipa_cold(e)	0	0	*rpiA*
EX_lipa(e)	0	0	*rpiA*
EX_enlipa(e)	0	0	*rpiA*
EDD	0	0, 100[i]	*tpiA*,*gnd-pgi*
PSK[j]	0	0, 100[k]	Tal
SBA[j]			Tal
TKT1			*tktA*[l]
TKT2			*tktA*[l]

[a]: no change if not shown
[b]: no change if not shown
[c]: adjusted to match the growth of single mutant indicated or the reason described in [d] and [e].
[d]: thrmodynamic constraint, limiting flux toward the direction of carbon source
[e]: induced on the carbon source
[f]: difference from the condition shown in A. Based on the information in Feist et al, 2007.
[g]: difference from the condition shown in A
[h]: 0.5 in tpiA mutant
[i]: 100 in gnd mutant
[j]: The new reactions from S7P to EHAP and E4P
[k]: 100 in Tal mutant
[l]: A minor isozyme (*tktB*), which was removed in the first FBA was added.